Modifications of Human Growth Differentiation Factor 9 to Improve the Generation of Embryos From Low Competence Oocytes

Jing-Jie Li, Satoshi Sugimura, Thomas D. Mueller, Melissa A. White, Georgia A. Martin, Lesley J. Ritter, Xiao-Yan Liang, Robert B. Gilchrist, and David G. Mottershead

Center of Reproductive Medicine (J.-J.L., X.-Y.L.), the Sixth Affiliated Hospital, Sun Yat-sen University, Guangzhou 520655, China; Institute of Agriculture (S.S.), Department of Biological Production, Tokyo University of Agriculture and Technology, Tokyo 183-0057, Japan; Robinson Research Institute (J.-J.L., S.S., M.A.W., G.A.M., L.J.R., R.B.G., D.G.M.), School of Paediatrics and Reproductive Health, The University of Adelaide, Adelaide 5005, Australia; Discipline of Obstetrics and Gynaecology, School of Women's and Children's Health (R.B.G.), Royal Hospital for Women, University of New South Wales, Sydney, New South Wales 2031 Australia; and Department of Plant Physiology and Biophysics (T.D.M.), Julius-von-Sachs Institute of the University Wuerzburg, 97082 Wuerzburg, Germany

Growth differentiation factor 9 (GDF9) is an oocyte-derived growth factor that plays a critical role in ovarian folliculogenesis and oocyte developmental competence and belongs to the TGF-β family of proteins. Recombinant human GDF9 (hGDF9) is secreted in a latent form, which in the case of the fully processed protein, has the proregion noncovalently associated with the mature region. In this study, we investigated a number of amino acid residues in the mature region of hGDF9 that are different from the corresponding residues in the mouse protein, which is not latent. We designed, expressed, and purified 4 forms of chimeric hGDF9 (M1–M4) that we found to be active in a granulosa cell bioassay. Using a porcine in vitro maturation model with inherent low developmental competence (yielding 10%–20% blastocysts), we tested the ability of the chimeric hGDF9 proteins to improve oocyte maturation and developmental competence. Interestingly, one of the chimeric proteins, M3, was able to significantly increase the level of embryo production using such low competence oocytes. Our molecular modeling studies suggest that in the case of hGDF9 the $Gly^{391}Arg$ mutation probably increases receptor binding affinity, thereby creating an active protein for granulosa cells in vitro. However, for an improvement in oocyte developmental competence, a second mutation ($Ser^{412}Pro$), which potentially decreases the affinity of the mature region for the proregion, is also required. **(*Molecular Endocrinology* 29: 40–52, 2015)**

The basic functional unit of the ovary is the ovarian follicle, consisting of an oocyte surrounded by cumulus, granulosa, and thecal cells. The oocyte is a central regulator of follicular function and plays a critical role in the regulation of follicle development, ovulation rate, and fecundity (1–3). Conversely, oocyte development is highly dependent on the surrounding cumulus cells for a supply of essential metabolic substrates and regulatory molecules (3, 4). Specific oocyte-secreted factors (OSFs) form the basis of a complex bidirectional communication network operating between cumulus cells and the oocyte (3). Growth differentiation factor 9 (GDF9) and bone morphogenetic protein 15 (BMP15) are 2 major OSFs. GDF9 and BMP15 target granulosa cells to regulate a

ISSN Print 0888-8809 ISSN Online 1944-9917
Printed in U.S.A.

Received June 3, 2014. Accepted November 11, 2014.
First Published Online November 13, 2014

Abbreviations: BMP15, bone morphogenetic protein 15; CEI, cumulus expansion index; COC, cumulus oocyte complex; 3D, 3-dimensional; GDF9, growth differentiation factor 9; HEK293T, human embryonic kidney 293T; hGDF9, human growth differentiation factor 9; IMAC, immobilized metal affinity chromatography; IVF, in vitro fertilization; IVM, in vitro maturation; mGDF9, mouse growth differentiation factor 9; OSF, oocyte-secreted factor; PDB, Protein Data Bank; mPZM-5, modified PZM-5.

broad range of cumulus cell and mural granulosa cell functions such as promoting granulosa cell proliferation (5), regulating cumulus expansion (6), progesterone synthesis (7, 8), and metabolism (9, 10), and preventing cumulus luteinization (11) and apoptosis (12, 13).

GDF9 is a well-known OSF (14–16), which plays a vital role in maintaining female fecundity. Any alteration in GDF9 expression and/or activity may lead to infertility or reproductive abnormalities (17). Consequently, genetic deletion of GDF9 leads to complete infertility in female mice (16). Similarly, inactivating mutations in GDF9 in sheep cause sterility in homozygous animals (18). Aberrant expression of GDF9 in the human is associated with diminished ovarian reserve (14), a poor response to ovarian stimulation (19), premature ovarian failure (20, 21), polycystic ovary syndrome (22, 23), and dizygotic twinning (24, 25).

Like other members of the TGF-β superfamily, GDF9 is produced as a precursor molecule consisting of an N-terminal proregion and a C-terminal mature region (26–28). It appears that the mature region of GDF9 is secreted from the oocyte in vivo along with the proregion, as most of the immunoreactive GDF9 from in vivo sources appears to be the unprocessed, noncleaved proprotein (29, 30). This finding suggests that an important point of control of the bioactivity of GDF9 in vivo may be the proteolytic processing of the protein after secretion from the oocyte. When recombinant GDF9 is produced in human embryonic kidney 293T (HEK293T) cells, most of the protein is secreted in the processed form, ie, cleaved at the "furin-like" processing site (28). Although the secreted GDF9 is processed, the proregion interacts noncovalently with the mature region to maintain GDF9 in a dimeric pro-mature complex (28, 31). The continued presence of the prodomain is likely to be essential for the stability of the GDF9 mature region (32, 33). Whereas hGDF9 is secreted in a latent form not capable of activating the GDF9 receptor, mouse GDF9 (mGDF9) is secreted from HEK293T cells in an active form (28, 31). Recently, it has been shown that when the glycine residue at position 391 of the hGDF9 sequence is replaced by an arginine (as found in the mGDF9 sequence) a GDF9 variant protein that is no longer latent is obtained (31).

In vitro maturation (IVM) of oocytes is a reproductive technology that eliminates or substantially reduces the use of stimulatory gonadotropin hormones in infertility treatment. However, the success rate for obtaining embryos derived from in vitro matured oocytes is far from comparable to that of in vivo matured oocytes, the pregnancy rate after IVM being less than half of the pregnancy rate after in vitro fertilization (IVF) procedures (34). Acquisition of developmental competency in cumulus oocyte complexes (COCs) is under the control of endocrine hormones and OSFs. IVM COCs are removed from the natural follicular environment, compromising oocyte-somatic cell interactions such that IVM COCs are deficient in BMP15 (35) and possibly GDF9. This finding is consistent with the many studies that have shown that supplementing IVM media with native OSFs or recombinant GDF9 and/or BMP15 significantly improves oocyte quality, post-IVF embryo development, and pregnancy outcomes (36–42). Until now, however, we have not been able to improve oocyte developmental competence by the addition of hGDF9.

In this study, we have made a number of mouse/human GDF9 chimeric proteins to produce a form of hGDF9 suitable for use in IVM medium development. We find that although the $Gly^{391}Arg$ form of hGDF9 is potently bioactive in vitro on granulosa cells in monolayer culture, it is not active on intact porcine COCs. However, a different chimeric form of hGDF9, incorporating a further 2 amino acid substitutions from the mGDF9 mature region sequence, is active on COCs and significantly enhances oocyte developmental competence and embryo production. Our molecular modeling of the different hGDF9 chimeric forms suggests that for bioactivity in vitro on COCs the hGDF9 wild-type mature region needs to have an increased receptor affinity and a decreased affinity for the associated proregion.

Materials and Methods

Construction of expression plasmids

Expression cassettes encoding wild-type hGDF9 and chimeric forms of the GDF9 DNA sequence were synthesized (Genscript USA, Inc), incorporating the rat serum albumin signal sequence at the 5′ end followed by sequences encoding for His8 and StrepII affinity tags at the N terminus of the GDF9 proregion. The cDNA fragments were cloned into the pEF-IRES expression vector (43). The amino acid sequences coding for the various proteins under consideration in this study are shown in Figure 1 and Table 1, which together summarize the changes in the different chimeric forms of hGDF9, referred to as M1, M2, M3, and M4.

Transfection and selection of stable cell clones

HEK293T cells were obtained from the American Type Culture Collection and cultured in DMEM (Invitrogen) containing 10% fetal calf serum, 2 mM L-glutamine, 100 IU/mL penicillin (Sigma-Aldrich), and 100 μg/mL streptomycin. The GDF9 expression plasmids were transfected into HEK293T cells using Lipofectamine 2000 (Invitrogen) following the manufacturer's instructions. Stable cell lines were established via puromycin selection.

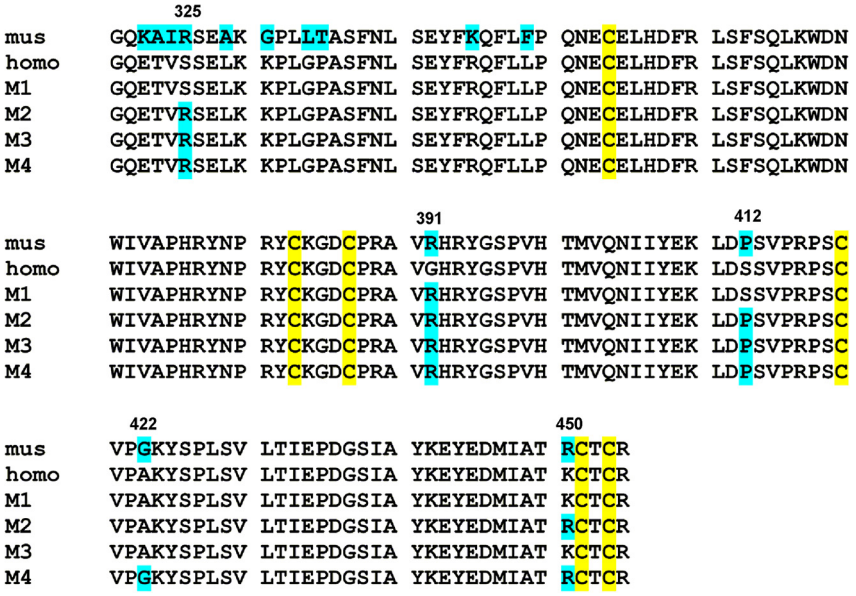

Figure 1. The mature region sequence alignment of wild-type mouse/human GDF9 and the chimeric GDF9 forms M1 to M4. The 6 conserved cysteine residues forming the cystine knot are shown in yellow, and the amino acid residues different from the wild-type human GDF9 sequence are shown in blue. Numbering is based on the human GDF9 amino acid sequence.

Nickel immobilized metal affinity chromatography (IMAC) purification

Cells producing wild-type hGDF9 or one of the mutant forms were grown to near confluence, and growth medium was then replaced by production medium containing DMEM/F12 GlutaMAX, 0.1 mg/mL BSA (Sigma-Aldrich), 25 IU/mL Fragmin (Pfizer), 100 U/mL penicillin, and 100 mg/mL streptomycin (Sigma-Aldrich). After 48 hours of incubation, the conditioned culture medium was collected and tested for the presence of the respective proteins by Western blotting using the GDF9 antibody (mAb53) (AbD Serotec). GDF9-containing conditioned medium (200 mL) was modified to include 10 mM imidazole, 500 μL protease inhibitor cocktail (Thermo Scientific), and 500 μL phosphatase inhibitor cocktail (Calbiochem) and subsequently adjusted to pH 7.4. Nickel-nitrilotriacetic acid agarose resin (1 mL; Invitrogen) was incubated with conditioned medium on a rotary agitator at 4°C for 2 hours and centrifuged at 900 rpm for 5 minutes, and the supernatant was removed. His-tagged GDF9 was eluted from the nickel-nitrilotriacetic acid agarose using elution buffer (PBS-500 mM imidazole) and stored in LoBind tubes (Eppendorf) at −80°C.

Silver staining, Western blotting, and quantification

IMAC purified samples were prepared for electrophoresis by mixing 10 μL of the sample with 5 μL of Tris-buffered saline and 5 μL of 4× SDS-PAGE loading buffer with 4 mM dithiothreitol. All samples were heated at 95°C for 5 minutes and then loaded onto a Mini-PROTEAN TGX 4%–15% gel (Bio-Rad Laboratories). After 40 minutes at 150 V, the gels were used for silver staining and Western blotting. Silver staining was performed following the manufacturer's instructions using a silver quest staining kit (Invitrogen). For Western blotting, proteins were transferred to a Hybond-ECL membrane (GE Healthcare) for 75 minutes at 100 V. Membranes were blocked with 2% blocking reagent (supplied in an ECL Advance Kit; GE Healthcare) diluted in Tris-buffered saline containing 0.1% (v/v) Tween 20 for 1 hour at room temperature. Subsequently, the membranes were incubated with anti-GDF9 antibody (mAb53) diluted 1:5000 at 4°C overnight, followed by incubation with goat anti-mouse IRDye 800 CW antibody diluted 1:10 000, for 1 hour in the dark. Fluorescence levels were determined using an Odyssey infrared imaging system (LiCor Biosciences). The IMAC purified promature GDF9 was quantified via Western analysis relative to recombinant mGDF9 standards (R&D Systems).

Table 1. Changes in the Different Chimeric Forms of hGDF9 M1 to M4

hGDF9 Chimera	Mutated Amino Acid Residues
M1	G391R
M2	S325R, G391R, S412P, K450R
M3	S325R, G391R, S412P
M4	S325R, G391R, S412P, A422G, K450R

Granulosa cell bioassay

Bioactivity testing of the various GDF9 chimeras was conducted using the mouse mural granulosa cell [^{3}H]thymidine incorporation bioassay, as described previously (5, 29). Mice were maintained in accordance with the Australian Code of Practice for Care and Use of Animals for Scientific Purposes and with the approval of the Adelaide University Animal Ethics Committee. 129/SV mice (21–26 days old) were injected with 5 IU of equine chorionic gonadotropin (Folligon; Intervet) and killed 44 to 46 hours later, and their ovaries were collected in warm Hepes-buffered TCM-199. Large antral follicles were punctured with a 27-gauge needle. Large clumps of granulosa cells were removed, and all COCs and denuded oocytes were discarded. Granulosa cells were washed and resuspended in bicarbonate-buffered TCM-199 supplemented with 0.3 mg/mL polyvinyl alcohol, 100 U/mL penicillin G, and 100 μg/mL streptomycin sulfate and plated in 96-well plates (Falcon; Becton Dickinson) at a density of 25 000 granulosa cells per well in a final volume of 125 μL. Cells were cultured in the presence of increasing concentrations (12.5–200 ng/mL) of wild-type or mutant hGDF9 (M1, M2, M3, or M4) or wild-type mGDF9 (R&D Systems) in an atmosphere of 37°C and 96% humidity in 5% CO_2 in air for 18 hours. The recombinant mGDF9 was supplied as a homodimer of the isolated mature region (ie, lacking the prodomain) and was included as a positive control. The cells were further exposed to a 6-hour pulse of 15.4 kBq [^{3}H]thymidine (PerkinElmer) under the same culture conditions. The incorporated [^{3}H]thymidine level was assessed using a Wallac Microbeta^2 plate counter after harvesting onto a filter mat using a Tomtec cell harvester. Each treatment was performed in duplicate, and the experiment was repeated 3 times.

Oocyte collection, in vitro maturation, and cumulus expansion assay

We were interested in the capacities of our various hGDF9 chimeras (M1–M4) to support oocyte maturation in vitro. Such an experiment is particularly difficult to perform in humans because of the extreme shortage of human oocytes for research. Because mouse oocytes are inherently developmentally competent, which poorly reflects the natural low developmental competence of human oocytes, we chose to investigate the effects of the GDF9 M1 to M4 proteins in a well-established low competence porcine IVM model (44). This IVM model uses COCs from growing small antral follicles (2–4 mm), collected from unstimulated gilts (peripubertal female pigs). Following best practice IVM and in vitro embryo production, these COCs typically yield at best 10% to 20% blastocysts (44).

Gilt ovaries were obtained from a local abattoir in 30 to 35°C physiological saline and then were washed and stored in saline at 38.5°C. COCs were aspirated from 2- to 4-mm diameter antral follicles using an 18-gauge needle and a syringe. PB1 medium (45) was used to wash and collect COCs. Compact COCs with more than 3 layers of cumulus cells and uniform ooplasm were chosen for IVM and placed in groups of 20 in 100-μL droplets of culture medium, porcine oocyte maturation basic IVM medium (46), supplemented with 1 mM dibutyryl cAMP and 100 ng/mL amphiregulin (R&D Systems) (47) for the first 22 hours of IVM. Subsequently, the COCs were transferred to another 100-μL droplet of culture medium for a further 22 hours in porcine oocyte maturation basic IVM medium without supplements. Cumulus expansion assays were performed, and the cumulus expansion index (CEI) was calculated as described previously (48, 49). In brief, a score of 0 suggests no visible response, a score of +1 shows cells in the peripheral 2 layers beginning to expand, a score of +2 displays expansion extending inwards to several layers, a score of +3 indicates expansion of nearly all layers of cumulus but not the corona radiata cells, and a score of +4 indicates expansion of the entire cumulus including corona radiata cells. Cumulus expansion was observed and scored at 22 hours of IVM.

In vitro embryo production and blastocyst staining

Fresh boar semen was purchased from Sabor Artificial Breeding Centre (Sabor Ltd). Semen was washed 3 times by centrifugation at 1500 × g and resuspended in PBS containing 1 mg/mL BSA for 5 minutes for each wash. Then the sperm were resuspended in IVF medium (50) and quantified. After IVM, 20 COCs were mechanically denuded and fertilized in IVF medium with semen at a final concentration of 5×10^5 sperm/mL at 38.5°C in 6% CO_2 for 1 hour. For embryo development, presumptive zygotes were cultured in modified PZM-5 (mPZM-5) (51), whereby 3 mg/mL BSA was used instead of polyvinyl alcohol. After fertilization, sperm were removed form oocytes/zygotes and washed 3 times in mPZM-5. A total of 20 oocytes/zygotes were transferred to a 100-μL droplet of mPZM-5 and cultured at 38.5°C in 7%O_2 and 6% CO_2 for another 7 days. Cleavage rates were assessed at day 2, and blastocyst rates were evaluated at day 7. After blastocyst rate assessment, blastocysts were incubated in ethanol containing 25 μg/mL Hoechst 33342 (Sigma-Aldrich) for 5 minutes and then mounted in a drop of glycerol in PBS on a microscope slide and covered by a coverslip. The total number of blastomeres were counted using a fluorescence microscope (TE 2000-E; Nikon) with a UV filter.

RNA isolation and RT-PCR analysis

After 22 hours of IVM, porcine COCs were mechanically stripped of their cumulus cells by vigorous pipetting using a 200-μL pipette. Cumulus cells from 40 COCs were lysed in 300 μL of RTL buffer containing 10 μL/mL 2-mercaptoethanol and stored at −80°C until RNA isolation. RNA isolation was performed by using an RNeasy Micro Kit according to the manufacturer's instruction (QIAGEN). The final RNA concentrations were determined using a NanoDrop spectrophotometer (Thermo Fisher Scientific). A total of 200 ng of RNA from each sample was reverse-transcribed using random primers (Invitrogen) by SuperScript III (Invitrogen Australia Pty Limited). The transcripts involved in cumulus expansion, *HAS2* (hyaluronan synthase 2), *TNFαIP6* (TNF-α-induced protein 6), and *PTGS2* (prostaglandin endoperoxide synthase 2), were analyzed by real-time PCR as described previously (52). *PPIA* (peptidylprolyl isomerase A) gene was used as the endogenous housekeeping control (52), because expression of this gene is stable in porcine IVM (data not shown). Sequences of PCR primers used for quantitative RT-PCR are shown in Table 2. Quantitative real-time PCR was performed in a 20-μL volume consisting of 2.5 μL of each forward and reverse primer, 2 μL of nuclease-free water, 10 μL of SYBR Green PCR Master Mix (Applied Biosystems), and 3 μL of cDNA from each sample on a Corbett Rotor-Gene 6000 machine (QIAGEN) in triplicate. Gene expression was calculated using the standard curve method and is presented relative to a calibrator (control group) and normalized to the housekeeping gene *PPIA*.

Molecular modeling

Homology models for the proprotein of hGDF9 and the ligand-receptor complex of the mature domain of hGDF9 were obtained by manual model building using the structures of the proprotein of human TGF-β1 (Protein Data Bank [PDB] entry 3RJR) (53) and the ternary ligand-receptor complex of BMP2 (PDB entry 2H64) (54) or BMP2 alone (PDB entry 3BMP) (55) as templates. For modeling of the proprotein of hGDF9, the sequence alignment was taken from the data published by Shi et

Table 2. Sequences of Primers for Real-Time PCR

Gene Name	Primer Sequence (5′-3′)		GenBank Accession No.	Amplicon Size, bp
	Forward	Reverse		
HAS2	AGTTTATGGGCAGCCAATGTAGTT	GCACTTGGACCGAGCTGTGT	AB050389.1	101
TNFAIP6	AGAAGCGAAAGATGGGATGCT	CATTTGGGAAGCCTGGAGATT	NM_001159607.1	106
PTGS2	AGCAATTCCAATACCAAAACCGTAT	TGTACTCGTGGCCATCAATCTG	NM_214321.1	102
PPIA	CATTTGCACTGCCAAGACTGA	GGACCCAAAGCGCTCCAT	AY266299.1	103

al (53). For modeling of the mature region of hGDF9, a sequence alignment was performed using residues 320 to 454 of hGDF9 and residues 292 to 396 of human BMP2. Residues differing between template and target were exchanged using the tool ProteinDesign in the software package Quanta2008 (Accelrys). Deletions and insertions up to 6 residues were built manually. The 3-dimensional (3D) models were subsequently refined to remove bad van der Waals contacts and to improve backbone and side chain geometry. Clashes between side chains were removed or minimized by performing rotamer searches, and subsequent energy minimization was applied in a stepwise manner using only geometrical energy terms (force field CHARMM27). First energy minimization runs were applied by keeping backbone atoms fixed and restraining all other heavy atoms with a harmonic potential of 25 kcal $Å^{-2}$ mol^{-1}. The latter harmonic potential force was decreased by 5 kcal $Å^{-2}$ mol^{-1} after every 500 steps of energy minimization. For final minimization, only the Cα-carbon atoms were restrained, and all other atoms were minimized without harmonic restraints. The final models exhibit good backbone geometry and have no bad van der Waals contacts. The mutations leading to the chimera M1 to M4 were introduced into the models by exchanging the respective amino acid residues in silico using the tool ProteinDesign/Mutate in the software package Quanta2008.

Statistical analysis

Statistical analyses were conducted using SPSS 17.0 (SPSS Inc). Differences among groups were analyzed for statistical significance by using variance (ANOVA) followed by a least significant difference post hoc test. All percentage data were arcsine transformed before analysis by ANOVA. A value of $P < .05$ was considered significant.

Results

Production and purification of mouse/human GDF9 chimeras

The sequences of the mGDF9 and hGDF9 mature regions are aligned in Figure 1, along with the sequences of the 4 hGDF9 chimeras (M1–M4) characterized in this study. Wild-type hGDF9 and the 4 chimeric proteins M1 to M4 were all produced with a poly-His tag placed at the N terminus of the proregion and expressed in HEK293T cells, as described previously (9, 28, 33, 56, 57). Conditioned media were collected from cell lines individually expressing these proteins, and the respective pro-mature complexes were purified by Ni^{2+}-based IMAC chromatography. The eluted fractions from the different purifications (wild-type hGDF9, Supplemental Figure 1; mutants M1–M4, Figure 2) exhibited comparable purity levels. Each purified pro-mature complex migrated as 3 major species in SDS-PAGE, corresponding to the proprotein and the processed pro and mature forms (bands A, B and C, respectively) (Supplemental Figure 1 and Figure 2). The Western blot of the purified hGDF9 wild-type

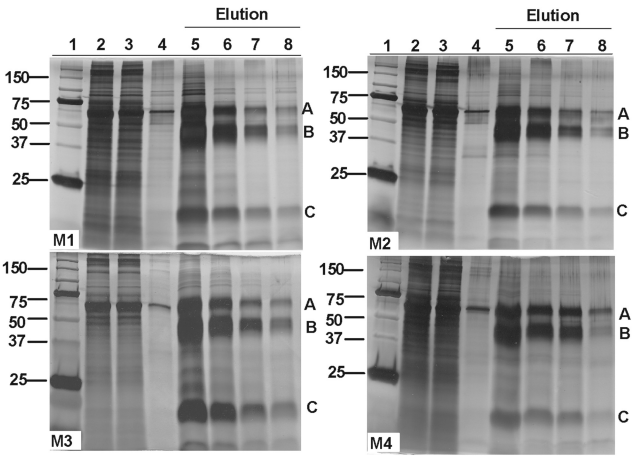

Figure 2. Silver-stained SDS-PAGE gels of mutant GDF9 (M1–M4) IMAC purification products: 1, molecular weight markers; 2, conditioned medium; 3, unbound material; 4, wash off no. 2; 5, elution no. 1; 6, elution no. 2; 7, elution no. 3; 8, elution no. 4. A, Proprotein form of GDF9. B, Processed proregion. C, Mature region.

pro-mature complex (Supplemental Figure 1) probed with an antibody specific for a peptide sequence in the GDF9 mature region is indicative of bands A and C being the unprocessed proprotein and mature region of GDF9, respectively. Similar results were obtained for the chimeric proteins M1 to M4 (data not shown). Whereas the four mutant forms of hGDF9 exhibited similar levels of purity (Figure 2), there was variation in the expression level and processing efficiency, with GDF9 M3 giving rise to the highest levels of processed mature region and M4 exhibiting the lowest processing efficiency.

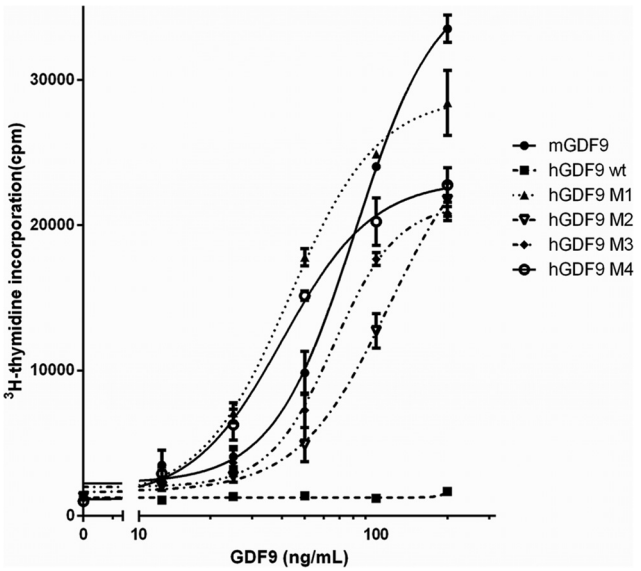

Figure 3. Bioactivity of the various human GDF9 forms on mouse mural granulosa cells. Granulosa cells were cultured with increasing concentrations (12.5–200 ng/mL) of recombinant mGDF9, IMAC-purified wild-type human GDF9, or one of the human mutant GDF9 forms, M1 to M4. The incorporated [^{3}H]thymidine was detected after a 24-hour incubation. Data points are the means ± SEM from 3 replicate experiments.

Human mutant GDF9 proteins are potently bioactive

We initially compared the activity of the hGDF9 forms M1 to M4 in a murine granulosa cell DNA synthesis bioassay. Figure 3 indicates that GDF9 M1 to M4 are all potently bioactive, as is recombinant mGDF9. The GDF9 M1 to M4 proteins can stimulate mural granulosa cell [^{3}H]thymidine incorporation at 12.5 ng/mL, and all hGDF9 chimeric proteins yielded marked dose-dependent increases in granulosa DNA synthesis. The GDF9 M1 protein is the most potent form in this assay compared with the other proteins. In contrast, as expected, wild-type hGDF9 had no effect on granulosa cell DNA synthesis (Figure 3). The M1 mutant was at least as bioactive as recombinant mGDF9 and approximately 2-fold more active than the GDF9 M2/M3 mutants. The Gly^{391}Arg mutation (the sole change in the M1 mutant) is thus the key mature domain residue to activate the latency of hGDF9 and appears in this study to produce a protein of bioactivity similar to that of mGDF9 in terms of murine granulosa cell DNA synthesis.

GDF9 M2 to M4 stimulate cumulus expansion and expression of the *TNFαIP6* gene in cumulus cells

Using a porcine oocyte low developmental competence model (44) as an appropriate experimental surrogate for the low developmental competency of human oocytes, we investigated the action of the hGDF9 M1 to M4 proteins on porcine COCs in terms of cumulus expansion and competency-related gene expression (Figure 4). After 22 hours of IVM, all groups exhibited only a moderate degree of cumulus expansion (CEI, <2.5), consistent with these COCs originating from small antral follicles. The hGDF9 M2, M3, and M4 proteins, but not the hGDF9 M1 form, enhanced the level of expansion significantly above that of the control (Figure 4). Consistent with morphological expansion (Figure 4A), hGDF9 M2, M3, and M4, but not M1, stimulated a significantly higher expression level of the *TNFαIP6* gene than the control or wild-type hGDF9-treated COCs (Figure 4B). However, none of the various hGDF9 forms had a significant effect on the expression level of the cumulus expansion–related gene *HAS2* or *PTGS2* (Figure 4, C and D).

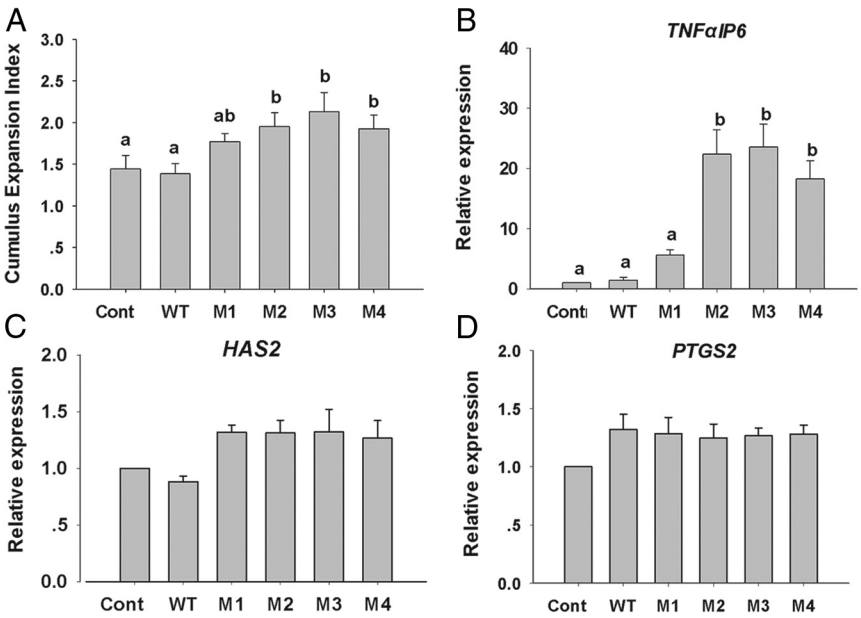

Figure 4. Porcine cumulus cell expansion and competency related gene expression. A, The CEI was evaluated after 22 hours of in vitro maturation with 200 ng/mL IMAC purified wild-type human GDF9 or one of the mutant human GDF9 forms, M1 to M4. Values represent the mean ± SEM of 5 replicates. After the CEI assessment, the expression levels of *TNFαIP6* (B), *HAS2* (C), and *PTGS2* (D) were examined by real-time RT-PCR analysis. Values represent means ± SEM of 3 replicates. Different letters indicate significant differences at $P < .05$. Cont, control.

GDF9 M3 enhanced embryo yield from oocytes with inherently low developmental competence

Following on from our cumulus expansion and competence–related gene expression experiment, we investigated the effect of the hGDF9 chimeric proteins on oocyte developmental competence and embryo production using oocytes with naturally low developmental competence. Porcine oocyte IVM medium was supplemented with human wild-type GDF9, M1, M2, M3, or M4 at a final concentration of 200 ng/mL, as this concentration gave clear responses for all chimeric proteins (M1–M4) in our granulosa cell bioassay (Figure 3). After fertilization, there were no significant differences in embryo cleavage rates between any of the groups (Figure 5A). GDF9 M3 significantly enhanced the blastocyst formation rate on day 7 by >2-fold from 17% (control) to 41% (GDF9 M3, $P < .05$) (Figure 5B). There was also a trend toward an improvement in blastocyst rate on day 7 from GDF9 M1, M2, and M4, but it was not statistically significant. The total blastocyst cell numbers on day 7 failed to show any significant differences between the groups (Figure 5C). However, the hatching blastocyst level on day 7 is also a good predictor of embryo viability and fetal developmental potential (58, 59), and we note that both GDF9 M2 and M3 significantly ($P < .05$) increased day 7 blastocyst hatching rates (Figure 5D).

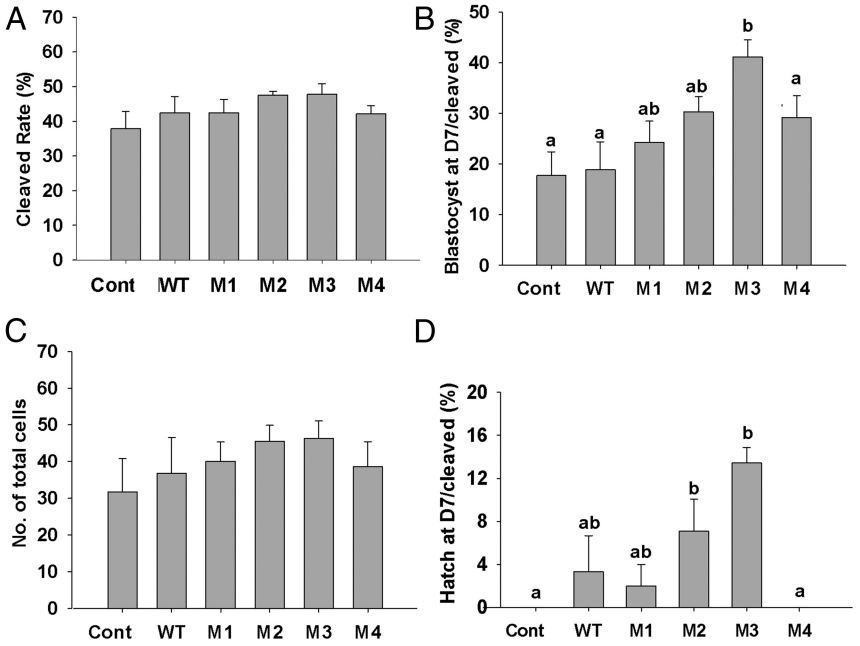

Figure 5. Effect of human GDF9 forms (wild-type and M1–M4) during porcine oocyte maturation on subsequent oocyte developmental competence. Porcine COCs with inherently low developmental competence were treated with vehicle, 200 ng/mL human wild-type GDF9 (WT), or one of the human mutant GDF9 forms (M1–M4) for the first 22 hours of IVM. The effects of treatments on oocyte development competence were examined by measuring the following points of embryo development: cleavage rate at day 2 (A), blastocyst rate expressed as a percentage of the number of cleaved embryos at day 7 (B), total blastocyst cell number on day 7 (C), and hatching blastocyst rate (number of hatching or hatched blastocysts/cleaved embryos) (D). All values are presented as means ± SEM from 5 replicate experiments. Different letters indicate significant differences at $P < .05$ within the same graph. Cont, control.

Molecular modeling of hGDF9 and variants

To obtain possible insights into the mechanisms by which the mutations incorporated into the M1 to M4 proteins affect GDF9 function, we performed homology modeling to derive 3D models for the proprotein complex, as well as a 3D model of the mature region of hGDF9 interacting with its type I and type II receptor ligand-binding domains. Modeling of the hGDF9 proprotein structure was performed in particular to identify potential influences of the different amino acid exchanges on the latency of hGDF9 and was performed by using the human pro-TGF-β1 structure as a template (53). Most of the proprotein of hGDF9 could be modeled except for the loop comprising residues His^{276} to Leu^{339}, which contains the conserved proteolytic processing site recognized by furin-like proteases. However, this loop, which also comprises a number of residues at the N terminus of the mature region differing between human and mouse GDF9, consists of mostly hydrophilic amino acid residues, and analysis tools predict a lack of regular secondary structure, suggesting that this loop is probably unstructured and flexible.

Using our hGDF9 proprotein model (Figure 6A) and inserting the mutations present in the mutants M1 to M4, we found that only residue Ser^{412} (mutated to proline in M2–M4) is near elements of the prodomain. In the model, residue Ser^{412} of hGDF9 shares contacts with residues located on helix α1, which is part of the straitjacket motif of the prodomain (53). Its exchange to a proline might thus disrupt/weaken the interaction with the neighboring residues, because proline cannot participate in similar hydrogen bonding. Furthermore, the proline ring possibly also introduces a steric hindrance due to the fact that the ring is oriented toward the straitjacket α-helix in the 3D model (Figure 6, B and C). Therefore, one explanation for the activity-altering effect of the mutation $Ser^{412}Pro$ might be a weakened interaction between the prodomain and the mature region in the GDF9 chimeras M2, M3, and M4. In contrast, the other mutations present in the different mutant GDF9 forms do not seem to directly contact elements of the prodomain and thus their influence on hGDF9 activity might be a result of altered receptor binding.

Hence, we also modeled the mature region of hGDF9 using BMP2 as a template and docked this model onto the complex of BMP2 bound to type I and type II receptors to analyze potential GDF9 ligand-receptor interactions (Figure 7A) (54). On the basis of our hGDF9 mature region ternary ligand-receptor complex model (Figure 7A), 2 amino acid exchanges present in the hGDF9 M1 to M4 chimeras are located near the potential type I receptor epitope of GDF9. The exchange of residue Gly^{391} in hGDF9 to the equivalent amino acid of murine GDF9, an arginine, led to a dramatic difference in protein activity (Ref. 31 and the present study). This residue is located in the so-called prehelix loop, which is a central and essential component in the ligand-type I receptor interaction of several BMPs and GDFs (60–64). The second amino acid of interest is Lys^{450} of hGDF9. Its exchange with an arginine, the equivalent amino acid in mGDF9, might also affect the GDF9-type I receptor interaction (Figure 7, D and E). Although the latter substitution seems conservative, analysis of the homology model indicates that the longer arginine side chain might engage in unique hydrogen bond interactions not possible with a lysine residue. This difference might then result in a difference in the

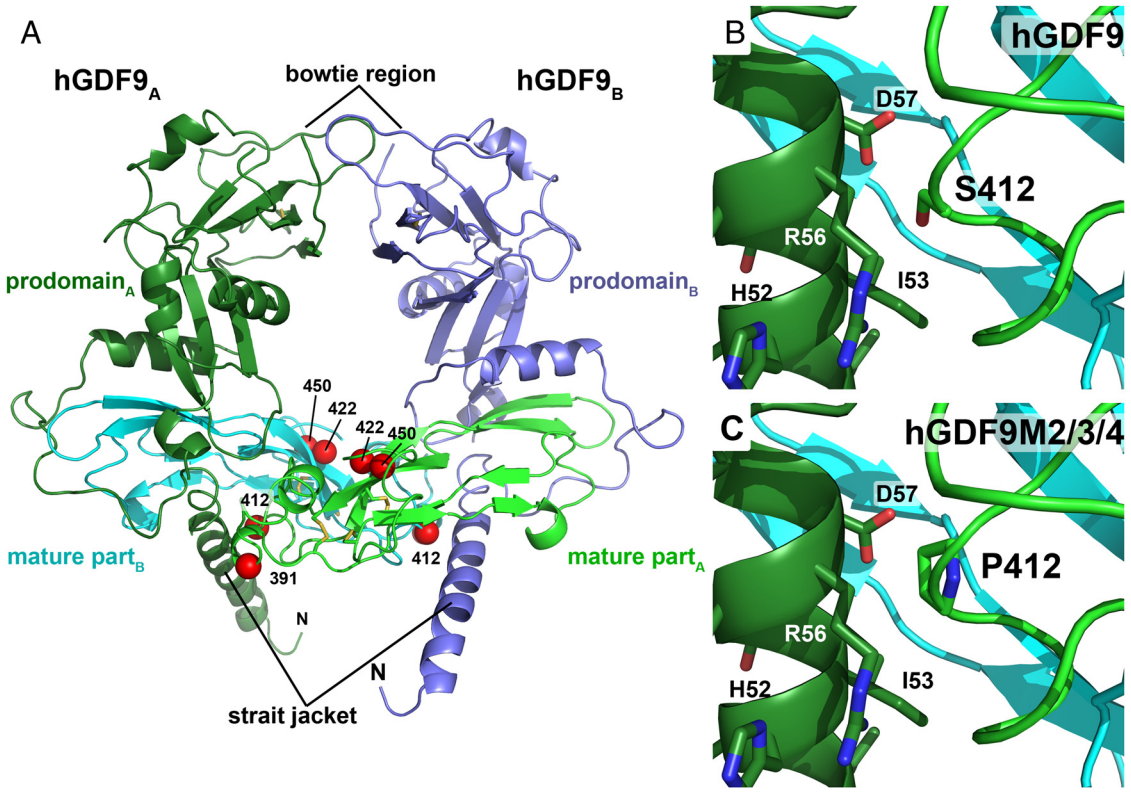

Figure 6. 3D homology model of the proprotein complex of human GDF9. The model was obtained using the crystal structure of pro-TGFβ1 as template. A, Ribbon plot of the homodimeric GDF9 colored in light/dark green (chain A) and blue/cyan (chain B). The mature region, which is released upon proteolytic processing of the proprotein at a conserved R-X-K/R-R site, is colored in light green and cyan. The prodomain engaging in a strait jacket–like interaction with the mature region, is marked in dark green and blue. The disulfide bonds of the characteristic cystine knot are shown as yellow sticks. Red spheres mark the Cα-carbon position of the mutations introduced to form the human-mouse GDF9 chimeras M1 to M4. B, Magnification around amino acid Ser^{412} located in the mature region of hGDF9 showing its close proximity to helix α1 of the prodomain. C, Exchange of Ser^{412} by proline, the equivalent residue in murine GDF9, possibly weakens this interaction and hence the pro/mature complex leading to a decreased latency for GDF9 chimeras M2 to M4.

conformation of the prehelix loop, which, as stated above, is an important element in the ligand-type I receptor interaction.

Discussion

A recent study by Simpson et al (31) showed that the single amino acid exchange of Gly^{391} to the corresponding residue found in the mGDF9 sequence (Arg) was sufficient to activate hGDF9 from the latent state. It appeared from the results of that study that although the Gly^{391}Arg mutant of hGDF9 was bioactive, it was not as potent as mGDF9. In the current study, it was our aim to engineer a form of hGDF9 to be as bioactive as mGDF9 via incorporation of various amino acid residue combinations from the mGDF9 mature region into the human sequence. Such a nonlatent mouse/human chimeric GDF9 protein could have application in the human artificial reproductive technology sphere.

Comparison of the mouse and human GDF9 mature region amino acid sequences shows that most of the differences are located in the flexible N-terminal region, before the cystine knot structure that is involved in receptor binding (Figure 1). In this study, with the exception of Ser^{325}, we have focused on those amino acid differences localized within the cystine knot structure. Previously, the phosphorylation status of Ser^{325} had been implicated in the level of bioactivity of hGDF9 (65, 66). In mGDF9, the corresponding amino acid is an arginine, which cannot be phosphorylated. Hence, in the hGDF9 chimeras M2 to M4 characterized in this study, we have incorporated the Ser^{325}Arg change as in the mouse protein to avoid any possible complications of phosphorylation status on the protein's bioactivity level. The protein GDF9 M1, with the single Gly^{391}Arg change, was produced to act as a point of comparison with the literature (31). Apart from the Ser^{325}Arg and Gly^{391}Arg changes, the mutant proteins M2 to M4 incorporate changes in one or more of the following amino acids: Ser^{412} (to Pro), Ala^{422} (to Gly), or Lys^{450} (to Arg). Alignment of the GDF9 mature region sequences across 9 different mammalian forms of this protein (Figure 8) clearly shows that the mutations we

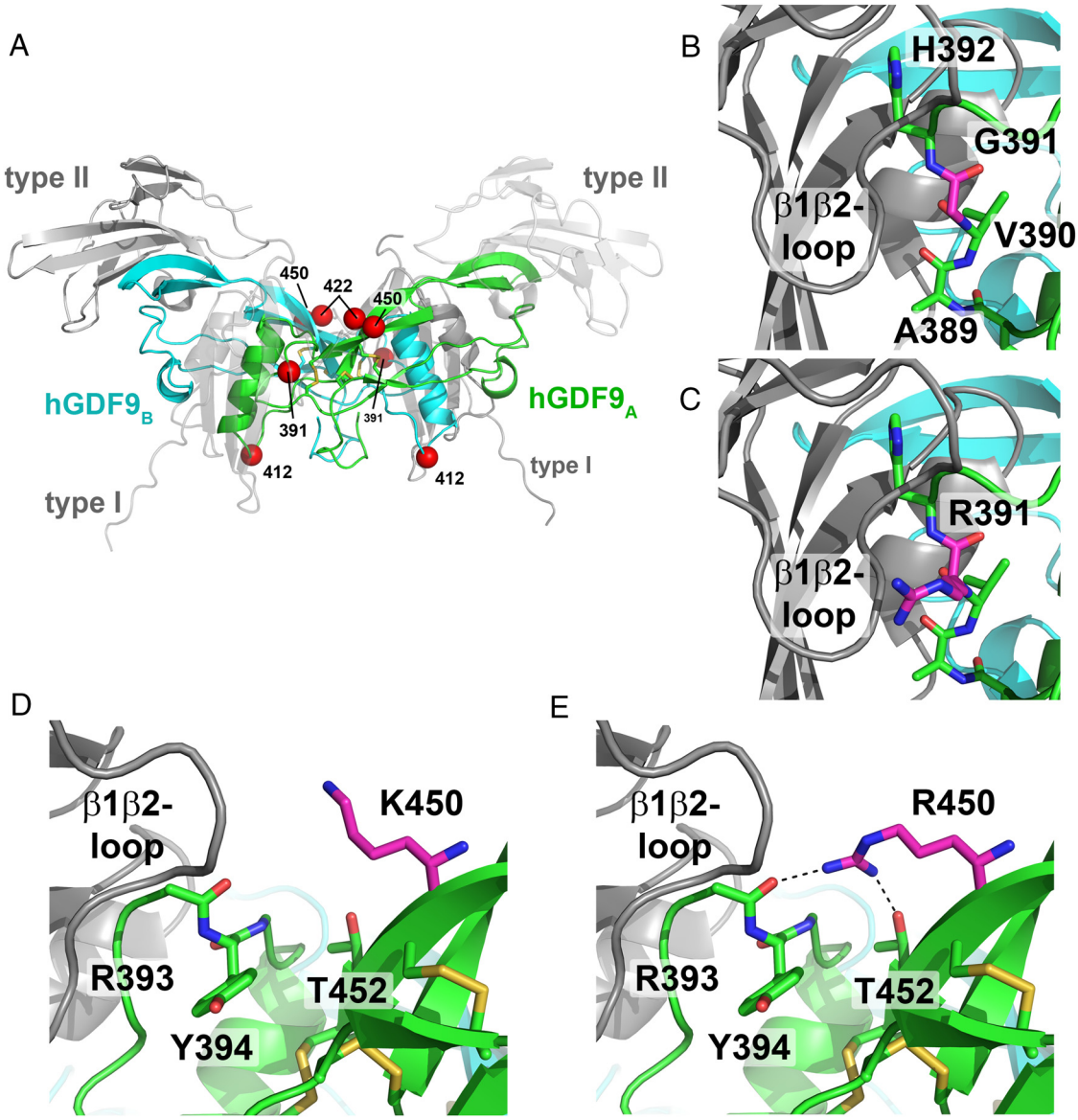

Figure 7. Homology model of the mature region of hGDF9 in complex with its type I and type II receptors. A, Overview ribbon plot of the hGDF9 dimer with the monomeric subunits colored in green and cyan. The potential receptor binding sites are indicated by gray ribbon structures for the type I and type II receptor ectodomains; for better visibility, the type I and the type II receptors facing the front are shown as transparent structures. Disulfide bonds of the cystine knot are shown as yellow sticks; the position of the residues exchanged to form the human-mouse chimera are indicated by red spheres. B and C, The residue at position 391 is located within the potential type I receptor binding site. Docking of a type I receptor to hGDF9 suggests that the residue at 391 is near the receptor's $\beta1\beta2$-loop, which was shown to be important in ligand-type I receptor interactions. In human GDF9, a small glycine residue occupies position 391 (B), whereas in mouse GDF9 a large positively charged arginine requires more space (C) but is capable of forming additional hydrogen bonds with the type I receptor. D and E, A second mutation in the human-mouse GDF9 chimera M2 and M4 is the exchange of Lys^{450} to arginine. As for the former substitution, this exchange could also enable additional interactions due to the longer side chain and the bidentate polar head group.

have incorporated into the M1 to M4 chimeric proteins are rodent-specific changes. Hence, we suggest that GDF9 in the other nonrodent species would also be produced in a latent form, similarly to hGDF9. Our modeling studies suggest that residues Gly^{391}, Ser^{412}, and Lys^{450} might be important for the level of bioactivity of hGDF9 either due to affecting the stability of the pro-mature complex or by possibly altering the receptor binding capabilities of mature GDF9. Recently, a similar molecular model was derived for pro-hGDF9 (17) by an automated modeling approach and used for the analysis of mutations occurring in human ovarian disorders.

As an initial characterization step of our purified chimeric hGDF9 proteins (M1 to M4), their bioactivity was compared with that of wild-type hGDF9 and a commercially available mGDF9 mature region in a murine granulosa cell proliferation assay. In this assay, the M1 form was the most potent GDF9 among the four chimeric

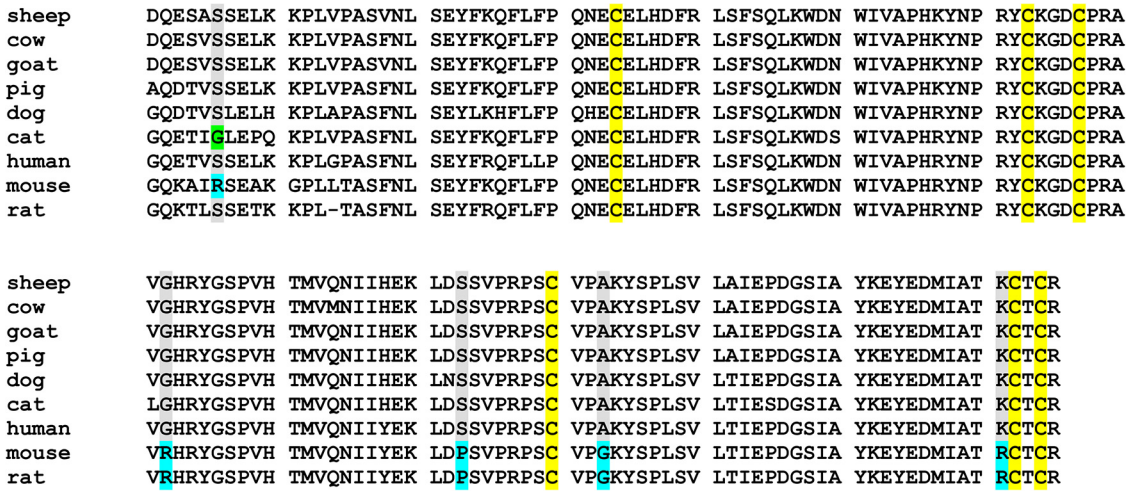

Figure 8. Alignment of 9 mammalian GDF9 mature region amino acid sequences. The residues targeted in this study are highlighted in blue within the mouse sequence, and a cat-specific change in one of these residues is highlighted in green. The Cys residues involved in formation of the conserved "cystine knot" structural element are highlighted in yellow.

forms and was at least as potent as the mGDF9 control. Previously, an analogous form of the GDF9 M1 protein was somewhat less potent than recombinant mGDF9 in this assay (31). This inconsistency could possibly be due to differences between the HEK293T host cells, the expression vector, or the purification protocols used in our study compared with those used previously. Wild-type hGDF9 was not active in this assay, as expected. Interestingly, the GDF9 M2 to M4 proteins show no increased bioactivity in this assay compared with that of GDF9 M1, even though they incorporate further mutations in addition to the $Gly^{391}Arg$ change. However, these results are consistent with our observation that the GDF9 M1 protein is already as active as mGDF9 in this bioassay.

We wanted to know what effects our various forms of purified hGDF9 would have on the level of developmental competency of COCs derived from small porcine follicles. This model was chosen because it resembles more closely the human oocyte, whereas murine COCs cannot be used because they are inherently competent. If a form of hGDF9 that would stimulate the developmental competency of such COCs could be produced, then this preparation could find application in the development of new forms of infertility treatment and fertility preservation for cancer patients. This is of relevance because the exogenous hormonal stimulation associated with standard IVF protocols can cause various adverse side effects, such as ovarian hyperstimulation syndrome and impaired endometrial receptivity (67, 68). Hence, IVM of oocytes is an attractive alternative for reducing or eliminating the administration of gonadotrophins in assisted reproductive technology. The use of oocytes cocultured with denuded oocytes has been an approach for supplying mixed OSFs, leading to significant improvements in oocyte developmental competence, embryo yield, and pregnancy rates in a range of animal models (36, 37, 39–42). Further, partially purified or crude recombinant GDF9 has also been used in a variety of studies to examine GDF9 bioactivity and IVM culture systems (29, 36–38, 69). However, for any use in the clinic, a purified protein preparation will be required. A commercially available purified form of hGDF9 has been used in a number of granulosa cell culture studies (70, 71). This form was bacterially produced, and the issue with any bacterially produced TGF-β family member is the question of what percentage of the refolded protein is correctly folded to supply the biologically active form (72). Further, being bacterially expressed, this hGDF9 lacks the posttranslational modifications that may be relevant for GDF9 (66, 72). Finally, the protein used for the above-mentioned granulosa cell studies consists of only the mature region of the protein, and we have recently shown that the purified mGDF9 mature region is not active in stimulating oocyte developmental competence (40). We have also shown for human BMP15 that the protein needs to be present as the purified pro-mature complex form to stimulate oocyte developmental competence (73). Hence, in our experiments, we have used the purified pro-mature complexes of hGDF9 and the related mutants.

We found that the purified wild-type hGDF9 pro-mature complex had no effect on oocyte developmental competence. This result could be anticipated because wild-type hGDF9 is reported to be produced in a latent form; however, it nonetheless demonstrates that the milieu of the cumulus cell extracellular matrix is also not capable of activating wild-type hGDF9. Intriguingly, the GDF9 M1 mutant (incorporating the activating $Gly^{391}Arg$ mutation [31]), which was particularly active in our mural granu-

losa cell bioassay, was not active in our cumulus expansion/gene expression experiments or in our oocyte developmental competence assay. In contrast to the M1 protein, we find that the GDF9 chimeras M2 to M4 all significantly increased cumulus expansion and the expression of the matrix-associated gene *TNFαIP6* but not the *HAS2* or *PTGS2* gene. The lack of an effect of GDF9 M2 to M4 on the latter 2 transcripts may be due to the specific culture conditions used, for example, the use of amphiregulin (74) or the time point at which expression levels were assessed.

Most importantly, we wish to highlight the fact that the GDF9 M3 chimera was capable of causing a >2-fold increase in oocyte developmental competence in our porcine low competence model. This result was also supported by a significant increase in the level of hatched embryos. The GDF9 M2 protein also showed a slight increase in these parameters, whereas the GDF9 M4 protein exhibited no difference compared with the control or M1. All 3 proteins (M2, M3, and M4 have the potentially important $Ser^{412}Pro$ change, which on the basis of our theoretical modeling of the proprotein complex, may decrease the affinity of the GDF9 mature region for the proregion. Of these 3 mutants we note that the GDF9 M3 protein maintains the second finger of the mature region as the wild-type human sequence, which may be of significance in terms of these competence results.

Overall, there is a clear difference between the GDF9 M1 protein and the M2 to M4 forms in that the GDF9 M1 protein is active on murine granulosa cells but had no effects that we could detect on porcine COCs. We speculate that, at least in the case of porcine COCs, a decreased affinity of the GDF9 mature region for the proregion (as we suggest the $Ser^{412}Pro$ change causes) is required for bioactivity, in addition to the $Gly^{391}Arg$ modification. Whether this is because of a murine/porcine species difference, a difference in the extracellular matrix, or receptor/coreceptor usage between mural and cumulus cells we cannot say at this stage.

With these results, we are the first to report that a purified form of hGDF9 (as the pro-mature complex) can improve oocyte developmental competence. Of particular significance is the fact that we have more than doubled embryo yield using oocytes that have poor developmental potential naturally. We chose this porcine low developmental competence model because a similar situation of poor developmental competence occurs for human oocytes after IVM in clinical practice (75). Hence, the ability of the GDF9 M3 protein to significantly improve developmental competence in the porcine model could make this form of hGDF9 a promising candidate for use in the development of an efficient clinical human IVM system.

Acknowledgments

Address all correspondence and requests for reprints to: David G. Mottershead, Robinson Research Institute, School of Pediatrics and Reproductive Health, The University of Adelaide, Adelaide 5005, Australia. E-mail: david.mottershead@adelaide.edu.au.

This work was supported by research grants and fellowships from the National Health and Medical Research Council of Australia (1017484 and APP1023210) and by grants from Cook Medical and Sun Yat-sen University, International Program Fund of 985 Project.

Disclosure Summary: R.B.G. is listed as an inventor on the patent US20140073052A1 owned by the University of Adelaide, has received speakers fees from Ferring and Merck Serono, consulting fees from Cook Medical, and research grant funding from Cook Medical. D.G.M. has received grant funding from Cook Medical and is listed on a distribution of benefits agreement in connection with patent US20140073052A1 owned by the University of Adelaide. The other authors have nothing to disclose.

References

1. **Wang XL, Wang K, Zhao S, Wu Y, Gao H, Zeng SM.** Oocyte-secreted growth differentiation factor 9 inhibits BCL-2-interacting mediator of cell death-extra long expression in porcine cumulus cell. *Biol Reprod*. 2013;89:56.
2. **Eppig JJ, Wigglesworth K, Pendola FL.** The mammalian oocyte orchestrates the rate of ovarian follicular development. *Proc Natl Acad Sci USA*. 2002;99:2890–2894.
3. **Gilchrist RB, Lane M, Thompson JG.** Oocyte-secreted factors: regulators of cumulus cell function and oocyte quality. *Hum Reprod Update*. 2008;14:159–177.
4. **Downs SM, Utecht AM.** Metabolism of radiolabeled glucose by mouse oocytes and oocyte-cumulus cell complexes. *Biol Reprod*. 1999;60:1446–1452.
5. **Gilchrist RB, Ritter LJ, Myllymaa S, et al.** Molecular basis of oocyte-paracrine signalling that promotes granulosa cell proliferation. *J Cell Sci*. 2006;119:3811–3821.
6. **Dragovic RA, Ritter LJ, Schulz SJ, Amato F, Armstrong DT, Gilchrist RB.** Role of oocyte-secreted growth differentiation factor 9 in the regulation of mouse cumulus expansion. *Endocrinology*. 2005; 146:2798–2806.
7. **Elvin JA, Yan C, Matzuk MM.** Growth differentiation factor-9 stimulates progesterone synthesis in granulosa cells via a prostaglandin E2/EP2 receptor pathway. *Proc Natl Acad Sci USA*. 2000; 97:10288–10293.
8. **Vanderhyden BC, Cohen JN, Morley P.** Mouse oocytes regulate granulosa cell steroidogenesis. *Endocrinology*. 1993;133:423–426.
9. **Sutton-McDowall ML, Mottershead DG, Gardner DK, Gilchrist RB, Thompson JG.** Metabolic differences in bovine cumulus-oocyte complexes matured in vitro in the presence or absence of follicle-stimulating hormone and bone morphogenetic protein 15. *Biol Reprod*. 2012;87:87.
10. **Su YQ, Sugiura K, Wigglesworth K, et al.** Oocyte regulation of

metabolic cooperativity between mouse cumulus cells and oocytes: BMP15 and GDF9 control cholesterol biosynthesis in cumulus cells. *Development*. 2008;135:111–121.
11. **Eppig JJ, Wigglesworth K, Pendola F, Hirao Y.** Murine oocytes suppress expression of luteinizing hormone receptor messenger ribonucleic acid by granulosa cells. *Biol Reprod*. 1997;56:976–984.
12. **Orisaka M, Orisaka S, Jiang JY, et al.** Growth differentiation factor 9 is antiapoptotic during follicular development from preantral to early antral stage. *Mol Endocrinol*. 2006;20:2456–2468.
13. **Hussein TS, Froiland DA, Amato F, Thompson JG, Gilchrist RB.** Oocytes prevent cumulus cell apoptosis by maintaining a morphogenic paracrine gradient of bone morphogenetic proteins. *J Cell Sci*. 2005;118:5257–5268.
14. **Wang TT, Ke ZH, Song Y, et al.** Identification of a mutation in GDF9 as a novel cause of diminished ovarian reserve in young women. *Hum Reprod*. 2013;28:2473–2481.
15. **Elvin JA, Clark AT, Wang P, Wolfman NM, Matzuk MM.** Paracrine actions of growth differentiation factor-9 in the mammalian ovary. *Mol Endocrinol*. 1999;13:1035–1048.
16. **Dong J, Albertini DF, Nishimori K, Kumar TR, Lu N, Matzuk MM.** Growth differentiation factor-9 is required during early ovarian folliculogenesis. *Nature*. 1996;383:531–535.
17. **Simpson CM, Robertson DM, Al-Musawi SL, et al.** Aberrant GDF9 expression and activation are associated with common human ovarian disorders. *J Clin Endocrinol Metab*. 2014;99:E615–E624.
18. **Hanrahan JP, Gregan SM, Mulsant P, et al.** Mutations in the genes for oocyte-derived growth factors GDF9 and BMP15 are associated with both increased ovulation rate and sterility in Cambridge and Belclare sheep (*Ovis aries*). *Biol Reprod*. 2004;70:900–909.
19. **Wang TT, Wu YT, Dong MY, Sheng JZ, Leung PC, Huang HF.** G546A polymorphism of growth differentiation factor-9 contributes to the poor outcome of ovarian stimulation in women with diminished ovarian reserve. *Fertil Steril*. 2010;94:2490–2492.
20. **Chand AL, Ponnampalam AP, Harris SE, Winship IM, Shelling AN.** Mutational analysis of BMP15 and GDF9 as candidate genes for premature ovarian failure. *Fertil Steril*. 2006;86:1009–1012.
21. **Dixit H, Rao LK, Padmalatha V, et al.** Mutational screening of the coding region of growth differentiation factor 9 gene in Indian women with ovarian failure. *Menopause*. 2005;12:749–754.
22. **Teixeira Filho F, Baracat EC, Lee TH, et al.** Aberrant expression of growth differentiation factor-9 in oocytes of women with polycystic ovary syndrome. *J Clin Endocrinol Metab*. 2002;87:1337–1344.
23. **Wang B, Zhou S, Wang J, et al.** Identification of novel missense mutations of GDF9 in Chinese women with polycystic ovary syndrome. *Reprod Biomed Online*. 2010;21:344–348.
24. **Palmer JS, Zhao ZZ, Hoekstra C, et al.** Novel variants in growth differentiation factor 9 in mothers of dizygotic twins. *J Clin Endocrinol Metab*. 2006;91:4713–4716.
25. **Montgomery GW, Zhao ZZ, Marsh AJ, et al.** A deletion mutation in GDF9 in sisters with spontaneous DZ twins. *Twin Res*. 2004;7:548–555.
26. **McPherron AC, Lee SJ.** GDF-3 and GDF-9: two new members of the transforming growth factor-β superfamily containing a novel pattern of cysteines. *J Biol Chem*. 1993;268:3444–3449.
27. **Hayashi M, McGee EA, Min G, et al.** Recombinant growth differentiation factor-9 (GDF-9) enhances growth and differentiation of cultured early ovarian follicles. *Endocrinology*. 1999;140:1236–1244.
28. **Mottershead DG, Pulkki MM, Muggalla P, et al.** Characterization of recombinant human growth differentiation factor-9 signaling in ovarian granulosa cells. *Mol Cell Endocrinol*. 2008;283:58–67.
29. **Gilchrist RB, Ritter LJ, Cranfield M, et al.** Immunoneutralization of growth differentiation factor 9 reveals it partially accounts for mouse oocyte mitogenic activity. *Biol Reprod*. 2004;71:732–739.
30. **McNatty KP, Lawrence S, Groome NP, et al.** Meat and Livestock Association Plenary Lecture 2005. Oocyte signalling molecules and their effects on reproduction in ruminants. *Reprod Fertil Dev*. 2006;18:403–412.
31. **Simpson CM, Stanton PG, Walton KL, et al.** Activation of latent human GDF9 by a single residue change ($Gly^{391}Arg$) in the mature domain. *Endocrinology*. 2012;153:1301–1310.
32. **Harrison CA, Al-Musawi SL, Walton KL.** Prodomains regulate the synthesis, extracellular localisation and activity of TGF-β superfamily ligands. *Growth Factors*. 2011;29:174–186.
33. **Watson LN, Mottershead DG, Dunning KR, Robker RL, Gilchrist RB, Russell DL.** Heparan sulfate proteoglycans regulate responses to oocyte paracrine signals in ovarian follicle morphogenesis. *Endocrinology*. 2012;153:4544–4555.
34. **Gremeau AS, Andreadis N, Fatum M, et al.** In vitro maturation or in vitro fertilization for women with polycystic ovaries? A case-control study of 194 treatment cycles. *Fertil Steril*. 2012;98:355–360.
35. **Mester B, Ritter LJ, Pitman JL, et al.** Oocyte expression, secretion and somatic cell interaction of mouse bone morphogenetic protein 15 during the peri-ovulatory period [published online ahead of print February 19, 2014]. *Reprod Fertil Dev*.
36. **Hussein TS, Thompson JG, Gilchrist RB.** Oocyte-secreted factors enhance oocyte developmental competence. *Dev Biol*. 2006;296:514–521.
37. **Hussein TS, Sutton-McDowall ML, Gilchrist RB, Thompson JG.** Temporal effects of exogenous oocyte-secreted factors on bovine oocyte developmental competence during IVM. *Reprod Fertil Dev*. 2011;23:576–584.
38. **Yeo CX, Gilchrist RB, Thompson JG, Lane M.** Exogenous growth differentiation factor 9 in oocyte maturation media enhances subsequent embryo development and fetal viability in mice. *Hum Reprod*. 2008;23:67–73.
39. **Romaguera R, Morató R, Jiménez-Macedo AR, et al.** Oocyte secreted factors improve embryo developmental competence of COCs from small follicles in prepubertal goats. *Theriogenology*. 2010;74:1050–1059.
40. **Sudiman J, Ritter LJ, Feil DK, et al.** Effects of differing oocyte-secreted factors during mouse in vitro maturation on subsequent embryo and fetal development. *J Assist Reprod Genet*. 2014;31:295–306.
41. **Dey SR, Deb GK, Ha AN, et al.** Coculturing denuded oocytes during the in vitro maturation of bovine cumulus oocyte complexes exerts a synergistic effect on embryo development. *Theriogenology*. 2012;77:1064–1077.
42. **Gomez MN, Kang JT, Koo OJ, et al.** Effect of oocyte-secreted factors on porcine in vitro maturation, cumulus expansion and developmental competence of parthenotes. *Zygote*. 2012;20:135–145.
43. **Hobbs S, Jitrapakdee S, Wallace JC.** Development of a bicistronic vector driven by the human polypeptide chain elongation factor 1α promoter for creation of stable mammalian cell lines that express very high levels of recombinant proteins. *Biochem Biophys Res Commun*. 1998;252:368–372.
44. **Marchal R, Vigneron C, Perreau C, Bali-Papp A, Mermillod P.** Effect of follicular size on meiotic and developmental competence of porcine oocytes. *Theriogenology*. 2002;57:1523–1532.
45. **Quinn P, Barros C, Whittingham DG.** Preservation of hamster oocytes to assay the fertilizing capacity of human spermatozoa. *J Reprod Fertil*. 1982;66:161–168.
46. **Yoshioka K, Suzuki C, Onishi A.** Defined system for in vitro production of porcine embryos using a single basic medium. *J Reprod Dev*. 2008;54:208–213.
47. **Procházka R, Petlach M, Nagyová E, Nemcová L.** Effect of epidermal growth factor-like peptides on pig cumulus cell expansion, oocyte maturation, and acquisition of developmental competence in vitro: comparison with gonadotropins. *Reproduction*. 2011;141:425–435.
48. **Vanderhyden BC, Caron PJ, Buccione R, Eppig JJ.** Developmental

pattern of the secretion of cumulus expansion-enabling factor by mouse oocytes and the role of oocytes in promoting granulosa cell differentiation. *Dev Biol*. 1990;140:307–317.
49. **Fagbohun CF, Downs SM.** Maturation of the mouse oocyte-cumulus cell complex: stimulation by lectins. *Biol Reprod*. 1990;42:413–423.
50. **Miyoshi K, Umezu M, Sato E.** Effect of hyaluronic acid on the development of porcine 1-cell embryos produced by a conventional or new in vitro maturation/fertilization system. *Theriogenology*. 1999;51:777–784.
51. **Suzuki C, Iwamura S, Yoshioka K.** Birth of piglets through the non-surgical transfer of blastocysts produced in vitro. *J Reprod Dev*. 2004;50:487–491.
52. **Gilchrist RB, Ritter LJ.** Differences in the participation of TGFB superfamily signalling pathways mediating porcine and murine cumulus cell expansion. *Reproduction*. 2011;142:647–657.
53. **Shi M, Zhu J, Wang R, et al.** Latent TGF-β structure and activation. *Nature*. 2011;474:343–349.
54. **Weber D, Kotzsch A, Nickel J, et al.** A silent H-bond can be mutationally activated for high-affinity interaction of BMP-2 and activin type IIB receptor. *BMC Struct Biol*. 2007;7:6.
55. **Scheufler C, Sebald W, Hülsmeyer M.** Crystal structure of human bone morphogenetic protein-2 at 2.7 A resolution. *J Mol Biol*. 1999;287:103–115.
56. **Pulkki MM, Myllymaa S, Pasternack A, et al.** The bioactivity of human bone morphogenetic protein-15 is sensitive to C-terminal modification: characterization of the purified untagged processed mature region. *Mol Cell Endocrinol*. 2011;332:106–115.
57. **Pulkki MM, Mottershead DG, Pasternack AH, et al.** A covalently dimerized recombinant human bone morphogenetic protein-15 variant identifies bone morphogenetic protein receptor type 1B as a key cell surface receptor on ovarian granulosa cells. *Endocrinology*. 2012;153:1509–1518.
58. **Van den Abbeel E, Balaban B, Ziebe S, et al.** Association between blastocyst morphology and outcome of single-blastocyst transfer. *Reprod Biomed Online*. 2013;27:353–361.
59. **Das ZC, Gupta MK, Uhm SJ, Lee HT.** Supplementation of insulin-transferrin-selenium to embryo culture medium improves the in vitro development of pig embryos. *Zygote*. 2014;22:411–418.
60. **Keller S, Nickel J, Zhang JL, Sebald W, Mueller TD.** Molecular recognition of BMP-2 and BMP receptor IA. *Nat Struct Mol Biol*. 2004;11:481–488.
61. **Kirsch T, Nickel J, Sebald W.** BMP-2 antagonists emerge from alterations in the low-affinity binding epitope for receptor BMPR-II. *EMBO J*. 2000;19:3314–3324.
62. **Kirsch T, Sebald W, Dreyer MK.** Crystal structure of the BMP-2-BRIA ectodomain complex. *Nat Struct Biol*. 2000;7:492–496.
63. **Kotzsch A, Nickel J, Seher A, et al.** Structure analysis of bone morphogenetic protein-2 type I receptor complexes reveals a mechanism of receptor inactivation in juvenile polyposis syndrome. *J Biol Chem*. 2008;283:5876–5887.
64. **Nickel J, Kotzsch A, Sebald W, Mueller TD.** A single residue of GDF-5 defines binding specificity to BMP receptor IB. *J Mol Biol*. 2005;349:933–947.
65. **Tibaldi E, Arrigoni G, Martinez HM, Inagaki K, Shimasaki S, Pinna LA.** Golgi apparatus casein kinase phosphorylates bioactive Ser-6 of bone morphogenetic protein 15 and growth and differentiation factor 9. *FEBS Lett*. 2010;584:801–805.
66. **McMahon HE, Sharma S, Shimasaki S.** Phosphorylation of bone morphogenetic protein-15 and growth and differentiation factor-9 plays a critical role in determining agonistic or antagonistic functions. *Endocrinology*. 2008;149:812–817.
67. **Lamazou F, Legouez A, Letouzey V, et al.** Ovarian hyperstimulation syndrome: pathophysiology, risk factors, prevention, diagnosis and treatment. *J Gynecol Obstet Biol Reprod (Paris)*. 2011;40:593–611. french
68. **Fatemi HM, Popovic-Todorovic B.** Implantation in assisted reproduction: a look at endometrial receptivity. *Reprod Biomed Online*. 2013;27:530–538.
69. **McNatty KP, Juengel JL, Reader KL, et al.** Bone morphogenetic protein 15 and growth differentiation factor 9 co-operate to regulate granulosa cell function in ruminants. *Reproduction*. 2005;129:481–487.
70. **Shi FT, Cheung AP, Leung PC.** Growth differentiation factor 9 enhances activin a-induced inhibin B production in human granulosa cells. *Endocrinology*. 2009;150:3540–3546.
71. **Huang Q, Cheung AP, Zhang Y, Huang HF, Auersperg N, Leung PC.** Effects of growth differentiation factor 9 on cell cycle regulators and ERK42/44 in human granulosa cell proliferation. *Am J Physiol Endocrinol Metab*. 2009;296:E1344–E1353.
72. **Mottershead DG, Watson AJ.** Oocyte peptides as paracrine tools for ovarian stimulation and oocyte maturation. *Mol Hum Reprod*. 2009;15:789–794.
73. **Sudiman J, Sutton-McDowall ML, Ritter LJ, et al.** Bone morphogenetic protein 15 in the pro-mature complex form enhances bovine oocyte developmental competence. *PLoS One*. 2014;9:e103563.
74. **Sugimura S, Ritter LJ, Sutton-McDowall ML, Mottershead DG, Thompson JG, Gilchrist RB.** Amphiregulin co-operates with bone morphogenetic protein 15 to increase bovine oocyte developmental competence: effects on gap junction-mediated metabolite supply. *Mol Hum Reprod*. 2014;20:499–513.
75. **Nogueira D, Sadeu JC, Montagut J.** In vitro oocyte maturation: current status. *Semin Reprod Med*. 2012;30:199–213.